Inorganica Chimica Acta, 35 (1979) 79–86
©Elsevier Sequoia S.A., Lausanne – Printed in Switzerland

Bismethyl-imido-triphosphoric acid-pentakis-dimethylamide (TRIPA) Complexes of Lanthanide Perchlorates

RAYMOND P. SCHOLER

Institut de Chimie Minérale et Analytique, Université de Lausanne, 3, Place du Château, 1005 Lausanne, Switzerland

Received November 3, 1978

The first lanthanide complexes with a neutral tridentate phosphoryl compound are reported. The compounds have the general formula $[Ln(TRIPA)_3](ClO_4)_3$, *where Ln = La–Lu, Y and TRIPA =* $[(CH_3)_2N]_2P(O)N(CH_3)P(O)[N(CH_3)_2]N(CH_3)P(O)[N(CH_3)_2]_2$. *Their nine-coordinate complex structure undergoes some subtle changes as a function of ionic radius, which seem to be primarily due to conformational rearrangements in the ligand molecules. In solution the complexes are inert with respect to ligand exchange, but the still appreciable flexibility of the bound TRIPA molecule gives rise to intramolecular exchange effects.*

Introduction

Hexamethylphosphoramide (HMPA) has been known for quite some time for its excellent complexing ability, but, due to its size and geometry, it can form only four-coordinate species with most metal ions including such large cations as Ba^{2+} and In^{3+} [1]. Six-coordinate complexes are formed only with the larger trivalent cations, *i.e.* the rare earth ions [2].

Nonamethylimidodiphosphoramide (NIPA), which can be considered as consisting of two 'fused' HMPA units, however, yields six-coordinate complexes of the general formula $[M(NIPA)_3]^{n+}(ClO_4)_n$ for all metals except the very small Li^+ [1, 3]. The higher coordinating ability of NIPA is probably due to both the chelate effect and the lesser steric expansion of the NIPA molecule as compared to two neighbouring HMPA molecules.

Bismethylimido-triphosphoric acid-pentakis-dimethylamide (TRIPA), which can be considered as consisting of three 'fused' HMPA molecules, has been found to form six-coordinate species of the general formula $[M(TRIPA)_2]^{n+}X_n$ in the presence of non-coordinating anions, X^-, with both main group and d transition metal ions, M^{n+} [4]. In view of the propensity of HMPA to form higher-coordinate species with rare earth ions, we thought it worthwhile to study the complexing behaviour of TRIPA in the presence of lanthanide perchlorates. We wish to report here the first series of complexes featuring three coordinated TRIPA molecules: $[Ln(TRIPA)_3](ClO_4)_3$, where Ln = La–Lu, Y. From the subsequent discussion it will appear that all phosphoryl groups coordinate, giving thus a nine-coordinate complex species. This sheds a very interesting light on the steric requirements of the HMPA homologues, considering for instance that it was impossible to create an eight-coordinate species with NIPA.

Experimental

Starting Materials

Rare earth oxides >99.9% were obtained from Rare Earth Products Ltd and Fluka. Reagent grade solvents and organic chemicals, purchased from Fluka, were used throughout without further purification. Sodium hydride was used as a 55–60% suspension in oil (Fluka). Toluene was degassed prior to use.

Preparation of TRIPA

The ligand was prepared according to an outline provided by Louw and Sprangers [5] with only minor alterations.

$(CH_3)_2NP(O)Cl_2$ (I) was obtained by adding $(CH_3)_2NH\cdot HCl$ to a 6.5-fold excess of $POCl_3$ and refluxing the mixture to complete dissolution (20 h at ~120 °C) prior to distillation [6] (b.p. 80 - 86 °C; 18 mm).

$[(CH_3)_2N]_2P(O)Cl$ (II) was obtained by heating 1 mol of HMPA to 100 °C, adding ½ mol of $POCl_3$ before increasing and maintaining the temperature at 150 °C for 2 h and finally distilling *in vacuo* through a Vigreux column (b.p. 50 °C; 0.01 mm) [7].

Adding II slowly in a 1:2 molar ratio to a stirred ether solution of CH_3NH_2 at –5 °C and letting the mixture stand overnight at room temperature yielded $[(CH_3)_2N]_2P(O)NHCH_3$ (III), which was recovered by filtering off $CH_3NH_2\cdot HCl$ and removing the ether *in vacuo* [8].

0.48 mol of III was dissolved in 600 ml of dry toluene. The solution was degassed and kept under

TABLE I. Analytical Data.[a]

Compound	Ln	C	H	N	Cl
$[La(TRIPA)_3](ClO_4)_3$	8.19 (8.19)	25.54 (25.50)	6.62 (6.42)	17.21 (17.35)	6.57 (6.27)
$[Ce(TRIPA)_3](ClO_4)_3$	8.13 (8.26)	25.42 (25.49)	6.54 (6.42)	17.32 (17.34)	6.27 (6.27)
$[Pr(TRIPA)_3](ClO_4)_3$	8.25 (8.26)	25.46 (25.49)	6.51 (6.42)	17.15 (17.34)	6.49 (6.27)
$[Nd(TRIPA)_3](ClO_4)_3$	8.49 (8.48)	24.60 (25.42)	6.16 (6.40)	16.85 (17.30)	7.18 (6.25)
$[Sm(TRIPA)_3](ClO_4)_3$	8.80 (8.81)	24.83 (25.33)	6.26 (6.38)	16.96 (17.23)	6.11 (6.23)
$[Eu(TRIPA)_3](ClO_4)_3$	8.92 (8.89)	25.03 (25.31)	6.29 (6.37)	16.88 (17.22)	6.24 (6.22)
$[Gd(TRIPA)_3](ClO_4)_3$	9.14 (9.18)	25.00 (25.23)	6.23 (6.35)	16.94 (17.16)	6.38 (6.21)
$[Tb(TRIPA)_3](ClO_4)_3$	9.19 (9.26)	24.89 (25.21)	6.20 (6.35)	16.78 (17.15)	5.94 (6.20)
$[Dy(TRIPA)_3](ClO_4)_3$	9.44 (9.45)	25.60 (25.15)	6.37 (6.33)	16.73 (17.11)	6.18 (6.19)
$[Ho(TRIPA)_3](ClO_4)_3$	9.48 (9.58)	25.80 (25.12)	6.41 (6.32)	16.44 (17.09)	6.18 (6.18)
$[Er(TRIPA)_3](ClO_4)_3$	9.72 (9.70)	25.65 (25.08)	6.31 (6.32)	16.43 (17.06)	6.06 (6.17)
$[Tm(TRIPA)_3](ClO_4)_3$	9.65 (9.79)	25.50 (25.06)	6.53 (6.31)	16.34 (17.05)	6.31 (6.16)
$[Yb(TRIPA)_3](ClO_4)_3$	9.97 (10.01)	24.90 (25.00)	6.16 (6.29)	16.86 (17.01)	6.17 (6.15)
$[Lu(TRIPA)_3](ClO_4)_3$	10.05 (10.11)	24.97 (24.97)	6.27 (6.29)	16.83 (16.99)	6.01 (6.14)
$[Y(TRIPA)_3](ClO_4)_3$	5.30 (5.40)	26.00 (26.28)	6.51 (6.62)	17.70 (17.88)	6.18 (6.46)

[a] Found (calculated) (%).

Ar. An equivalent amount of NaH was added portionwise under vigorous stirring. The mixture, containing essentially $[(CH_3)_2N]_2P(O)N(CH_3)Na$, was then left standing for about 5 h, upon which a degassed solution of 0.25 mol of I in 200 ml of dry toluene was slowly added under stirring. The resulting solution was rapidly heated to boiling and allowed to cool to room temperature. NaCl was then filtered off under Ar and toluene removed by distillation. The oily residue was washed with dry diethyl ether and the remaining white solid, TRIPA, dried *in vacuo*. M.p. 114 °C, yield: 35–40%. ^{31}P-NMR (d_6-acetone, ext. ref. 62.5% H_3PO_4): δ = 15.45 ppm (triplet), 18.96 ppm (doublet); J_{P-P} = 17.65 Hz.

Preparation of the Rare Earth Perchlorates

The dry rare earth perchlorates were obtained by dissolution of the corresponding oxides Ln_2O_3 in a stoichiometric amount of 30% perchloric acid, followed by evaporation to dryness *in vacuo* (10^{-5} mm).

Cerium(III) perchlorate was prepared from $CeCl_3 \cdot 6H_2O$: the chloride was dissolved in a minimum excess of 60% $HClO_4$ and the solution was gently heated at reduced pressure till completion of HCl evolution. Evaporation of H_2O at 10^{-2} mm yielded an oily precipitate (containing excess $HClO_4$ [9]), which was recrystallized 3 times from H_2O. The salt was dried at 10^{-5} mm (2–3 days).

Preparation of the Complexes

A dry acetone solution of TRIPA was added in a 4:1 molar ratio to a dry acetone solution of $Ln(ClO_4)_3$. A faint precipitate formed immediately, in a few cases only after addition of a few drops of dry diethyl ether. The solution was allowed to settle overnight in the refrigerator. The precipitate was then filtered off and washed several times with small amounts of dry acetone to remove excess TRIPA. After recrystallisation from acetone the complex was kept at 10^{-5} mm for several days prior to analysis and stored under Ar. Yields varied between 50% and 70%. All complexes were analysed as $[Ln(TRIPA)_3](ClO_4)_3$ (Table I) and handled in a dry-box for all subsequent measurements.

Analytical Measurements

The metal content of the complex was assessed by complexometric titration with 2×10^{-3} *M* $(NH_4)_3H(EDTA)$ in the presence of urotropine as buffer and xylene orange as indicator [10]. Microanalytical determinations of C, H, N and Cl were performed by W. Manser, Mikrolabor, ETH, Zurich. IR spectra proved the absence of water in the complexes.

Physical Measurements

Powder diffraction spectra were obtained on a Huber Guinier type camera equipped with a Johann graphite monochromator using CuK_α radiation. Infrared spectra in the 4000–200 cm^{-1} region were recorded on a Perkin-Elmer 577 grating IR spectrophotometer. The solid samples were mulled in nujol and placed between CsBr plates. Raman data in the 3200–50 cm^{-1} region were obtained with a SPEX 1403 CompAct spectrophotometer using the 5145 Å line of an argon ion laser (Spectra Physics 164) as the excitation source and ordinary capillary tubes as sample recipients.

TABLE II. Infrared and Raman Bands (cm^{-1}) of Solid TRIPA and [Gd(TRIPA)$_3$](ClO$_4$)$_3$.

TRIPA		Assignment		[Gd(TRIPA)$_3$](ClO$_4$)$_3$	
IR[a]	Raman[b]	TRIPA	Perchlorate	IR[a]	Raman[b]
1230 vs	1228(5)	PO stretching		1198 vs, b	1196(3)
1216 s	1213(11)	CN stretching		c	1242(8)
				1223 sh, m	1220(1)
1190 vs, b	1194(8)	PO stretching		1180 m	1172(3)
		CN stretching			
1150 sh, m		CH_3 rocking		1150 m	
	1104(2)	CH_3 rocking			
			ν_3 (F_2) [T_d]	1091 s, b	1094(3)
1070 vs	1072(8)	CN stretching		1073 sh, w	1072(7)
				1050 m	
1012 sh, w	1010(4)	CH_3 rocking		1017 m	1014(3)
1004 sh, m		CH_3 rocking			
990 vs	995(9)	PN stretching		998 s	
	986(5)	PN stretching		993 sh, s	990(5)
			ν_1 (A_1) [T_d]	932 sh, w	927(100)
912 m	910(1)	PN stretching		908 s	905(14)
875 vs, b		PN stretching		885 s	
				874 s	
763 s		PN stretching		770 sh, w	
				766 m	
755 sh, m	754(4)	PN stretching		757 m	758(2)
	747(6)	PN stretching			743(17)
739 m	734(7)				
720 s	715(5)	PN stretching		730 m	
684 m	683(16)	PN stretching		688 m	
				680 m	683(9)
674 sh, w		PN stretching		673 sh, w	674(7)
627 m–s	622(1)	PN stretching		641 sh, w	635(10)
			ν_4 (F_2) [T_d]	628 vs	620(55)
595 w–m	595(100)	NPN bending		605 m	600(20)
520 sh, m	515(6)	CNP bending		518 sh, m	
				512 m	512(7)
508 s	504(4)	PO bending		534 vs	
484 m	476(2)	PO bending		492 m	484(3)
470 sh, m		CNP bending		474 m	
			ν_2 (E) [T_d]	460 sh, w	455(12)
434 m	431(4)	CNP bending		432 m	
420 vw				425 sh, vw	
415 vw	412(4)			410 vw	
396 m	391(8)	PNP bending		381 sh, w	
370 m	368(2)	CNC bending		368 m	364(2)
356 sh, m	349(6)	CNP bending		357 sh, w	346(1)
312 w	315(7)	CNP bending		321 sh, vw	
				307 w–m	
283 w	286(1)	CNP bending			
252 w	258(3)	CH_3 torsion		270 m	273(3)

[a] Abbreviations for band characteristics: 1st symbol (band intensity): vs = very strong; s = strong; m = medium; w = weak; vw = very weak; sh = shoulder. 2nd symbol (band width): b = broad. [b] Raman band intensities are given as percentages of the main peak. [c] Masked by PO stretching vibration.

80 MHz ^{1}H NMR spectra were recorded on a Bruker WP-80-CW spectrometer, 60 MHz ^{1}H NMR and ^{31}P NMR spectra (with broadband proton decoupling) were obtained respectively with a Bruker WP-60 FT spectrometer and a Bruker HX-90 spectrometer equipped with a BSV3 FT unit. Temperature stabilisation was guaranteed by means of a Bruker BST-100/700 variable temperature unit. Samples prepared for chemical shift measurements were *ca.* 10^{-1} *M* in the lanthanide complex. A capillary of

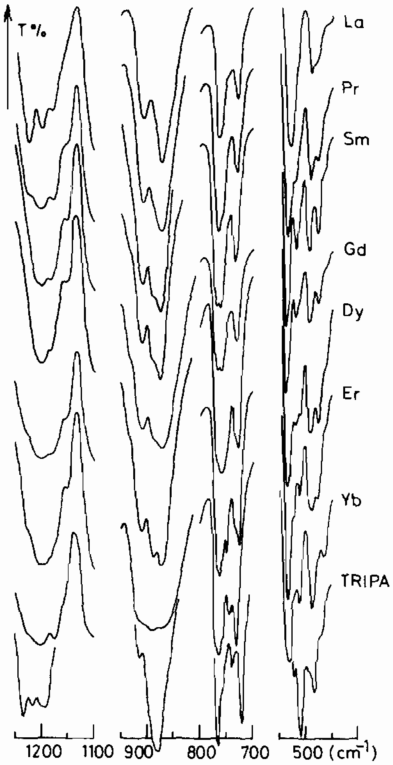

Fig. 1. Infrared spectra (1250–1100 cm^{-1}; 950–700 cm^{-1}; 550–450 cm^{-1}) of TRIPA and [Ln(TRIPA)$_3$]-(ClO$_4$)$_3$.

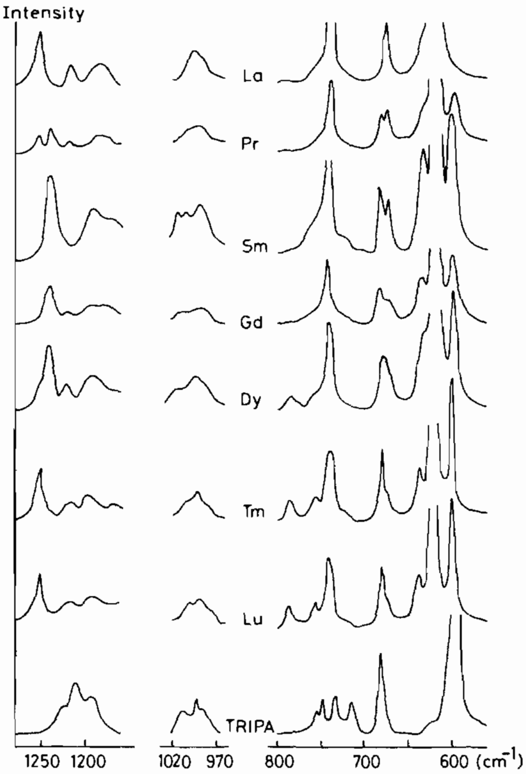

Fig. 2. Raman spectra (1280–1160 cm^{-1}; 1020–960 cm^{-1}; cm^{-1};800–560 cm^{-1}) of TRIPA and [Ln(TRIPA)$_3$](ClO$_4$)$_3$.

62.5% H_3PO_4 was used as external reference for ^{31}P measurements. $Si(CH_3)_4$ was used as internal reference in ^1H samples. Downfield chemical shifts are reported as positive.

Results and Discussion

Powder Diffraction Spectra

Although coordinating anions are absent (*vide infra*), the series [Ln(TRIPA)$_3$](ClO$_4$)$_3$ is not isomorphous. Five X-ray types can be distinguished: La–Ce (A), Pr–Nd (B), Sm–Eu (C), Gd–Er (D), Tm–Lu(E). The difference in line patterns for type B and C is rather small.

Vibration Spectra

Table II features the infrared and Raman data of solid TRIPA and [Gd(TRIPA)$_3$](ClO$_4$)$_3$ in the 1300–250 cm^{-1} region. The ligand vibrations observed at higher frequencies are not visibly influenced by coordination and are thus irrelevant to discussion. The tentative assignments of the TRIPA frequencies were made on the basis of the assignments for HMPA and NIPA vibrations by de Bolster and Groeneveld [11]. Figures 1 (IR) and 2 (Raman) give the only spectral regions where changes occur along the lanthanide series. The strong 1230 cm^{-1} IR band of free TRIPA does not show up in the spectra of the complexes nor is it replaced by a band at higher frequency. We must therefore assume that it has shifted to lower energy. Of the close lying CN and PO stretching vibrations in HMPA and NIPA, the former is shifted to higher energy and the latter to lower energy on coordination [11]. The PO shift amounts to 30–35 cm^{-1} in lanthanide–NIPA complexes [3]. We conclude that the 1230 cm^{-1} TRIPA band corresponds to a PO stretching frequency and that it is represented in the complexes by the broad absorption at ~1200 cm^{-1} (Fig. 1). In the Raman spectra a corresponding shift occurs from 1228 to 1184–1197 cm^{-1} (Fig. 2). The Raman CN band is usually more intense than the PO band [2], which suggests that the 1213 cm^{-1} (R) ligand band is a CN vibration which shifts on coordination to 1242–1254 cm^{-1}. The corresponding IR band is only plainly observed in the free ligand spectrum (1216 cm^{-1}), while it is probably hidden under the broad PO band in the complex spectra. The broad 1190 cm^{-1} (IR)/1194 cm^{-1} (R) band in the free ligand may be due to a combination of a PO and a CN stretching vibration. In the complexes it probably splits into the observable low energy band at 1175–1180 cm^{-1} (PO stretch) and a component at ~1200 cm^{-1} (CN stretch) masked by the main PO absorption. In view of the appreciable number of structural types along the series it would seem convenient to imagine the ligand coordinating in different ways which would depend largely on the ionic radius, *e.g.*, TRIPA could act occasionally as a bidentate ligand, maintaining one PO group out of the coordination sphere. This free PO group would account for the residual 1225 cm^{-1} (IR)/1223–1228 cm^{-1} (R) band in the complex spectra. However, the origin of this band could also lie in a splitting of the main CN stretching band. As the Raman spectra (Fig. 2) show, the 1125 cm^{-1} band is the more intense, the higher the frequency of the CN vibration. As the CN stretch shifts towards 1240 cm^{-1}, the 1225 cm^{-1} band gradually disappears. It is quite possible that the CN stretch actually splits into three components of varying intensity according to the overall complex structure. The Raman spectrum of the praseodymium complex is very significant in this respect in that it shows all three components with comparable intensities. The splittings (which can also be observed on other bands, *e.g.* the PN stretching vibrations, *cf.* Table II, Fig. 1 and 2) may be due to crystal packing forces or to complex-induced non-equivalence of CN bonds. These considerations together with the fact that the PO bending frequency (free ligand: 508 cm^{-1} (IR)/504 cm^{-1} (R)) remains constantly intense and shifted to higher frequencies (530–535 cm^{-1} (IR)/523–530 cm^{-1} (R)) in all complexes are in favour of all PO groups coordinating to lanthanide ions.

Of the four observed anion bands in the complex spectra (Table II), *i.e.*

a) 1088–1095 cm^{-1} (IR)/1088–1100 cm^{-1} (R)
b) 931–935 cm^{-1} (IR)/924–931 cm^{-1} (R)
c) 626–629 cm^{-1} (IR)/618–625 cm^{-1} (R)
d) 457–462 cm^{-1} (IR)/453–458 cm^{-1} (R),

(b) and (d) appear only as weak shoulders in the infrared and are sometimes missing altogether (Fig. 1). They would therefore correspond respectively to the ν_1 and ν_2 modes of ionic (T$_d$) perchlorate, as both these modes are infrared inactive [2]. (a) and (c) can then be assigned accordingly to the ν_3 and the ν_4 mode of the perchlorate anion. The spectra show thus clearly that the anions are not coordinating. The initial absence and conspicuous intensity increase of the 600 cm^{-1} Raman band (Fig. 2) along the lanthanide series could arise from a splitting of the ν_4 perchlorate mode, due to some preferred orienting of the anion as a result of crystal packing forces, but it can also be attributed to an intensification of the NPN bending mode as a consequence of the overall complex symmetry. In the absence of any further evidence to the contrary, we can therefore conclude that we deal with purely ionic perchlorate and that the solid TRIPA complexes can be formulated as 1:3 salts with a lanthanide coordination number of 9: [Ln(TRIPA)$_3$](ClO$_4$)$_3$.

The complex structure can probably be approximated by an ideal polyhedron at least for the complexes of the lighter lanthanides. ^{31}P NMR spectra of these complexes in CD$_2$Cl$_2$ (*vide infra*) show indeed only two kinds of phosphorus nuclei with a population ratio of 2:1. Structures of 9-coordinate complexes are always described in terms of the tricapped trigonal prism (TCTP) or the capped square antiprism (CSAP) [12]. Most known M(L–L–L)$_3$ molecules have essentially TCTP structure: the 3 tridentate ligands are equivalent, with the central donor atom occupying the capping position and the outer donor atoms occupying opposite sites in the capped quadrilateral face. It has been noted [12], however, that strict TCTP symmetry is only observed, if the ligand molecules have imposed planar geometry. If this is not the case, a distortion toward CSAP is usually found. From a CPK (Ealing Corp., Cambridge, Mass.) model of TRIPA it appears that some strain has to be imposed on the molecular geometry in order to put the outer oxygen atoms in opposite corners of a quadrilateral face. Consequently, the TRIPA complexes would have a structure somewhere between TCTP and CSAP. The amount of distortion depends probably on the radius of Ln^{3+} and would account for the different X-ray types observed in powder diagrams.

NMR Spectra

The ^{31}P NMR spectrum of TRIPA in CD$_2$Cl$_2$ at RT shows a doublet for the outer phosphorus atoms and a triplet for the central one at respectively 19.45 and 15.70 ppm (relative to 62.5% H$_3$PO$_4$) with $J_{P-P} = 17$ Hz. Both signals converge toward each other with decreasing temperature, but no change in their shape is visible at temperatures as low as –70 °C. This probably indicates fast chemical exchange between different conformations. CPK models suggest indeed that TRIPA may exist between two extreme conformations: a highly polar conformation A, with all three PO groups lying close together on the same side of the molecule and a less polar one, B, with the outer PO groups at opposite edges on one side of the molecule and the central PO group, well hidden among methyl groups, on the other side. In Table III are listed the shifts experienced at various temperatures by both ^{31}P signals on complexation to La^{3+} and Lu^{3+}.

The much greater shift experienced by the central P atom as compared to that of the outer P atoms cannot be explained by a mere bonding effect, since the central donor atom is normally farther away from the metal ion than the outer donor atoms. Nor can the difference in sign for the La^{3+} and the Lu^{3+} induced doublet shifts be accounted for without the assumption of a change in ligand conformation prior to coordination. We believe that B is the prevailing conformation of the free ligand in the rather unpolar

TABLE III. ^{31}P Complexation Shifts [ppm].

T [°C]	La^{3+}		Lu^{3+}	
	doublet	triplet	doublet	triplet
25			1.83	3.80
−10	−0.36	2.57		
−30	−0.30	2.79	1.15	3.94
−72	−0.20	2.83		

dichloromethane and that A is the conformation favoured in the complexes. If one accepts that the chemical shifts for conformation A lie somewhere between the corresponding shifts for conformation B, as seems to be indicated by the temperature dependence of the free ligand shifts, the different effects observed in Table III can easily be explained as shown in Fig. 3. Lutetium induces a greater complexation shift than lanthanum, not only on account of stronger bonding of the ligand to the smaller ion, but also because the pure A conformation may be sterically unfavourable with respect to the ionic size. The latter effect also explains the increase of the Lu-induced doublet shift with increasing temperature, as more and more "B-type" conformation is populated. This change in the conformation of the complexed ligand would be consistent with the structural changes observed in powder diffraction and vibration spectra as a function of decreasing ionic radius.

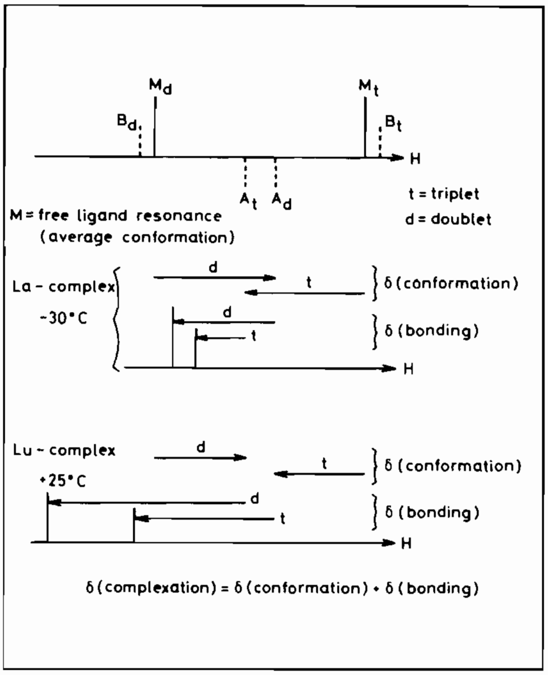

Fig. 3. Contributions to La and Lu induced ^{31}P complexation shifts.

^1H NMR spectra of TRIPA in CD_2Cl_2 at normal temperatures are characterized by three overlapping signals, which could be identified on the spectra recorded at 80 MHz: (a) a quartet at 2.76 ppm, due to coupling of the imido protons with the two neighbouring P atoms ($J_{P(central?)H}$ = 10.0 Hz, $J_{P(outer?)H}$ = 9.0 Hz), (b) a broad doublet at 2.71 ppm (J_{PH} = 9.0 Hz), composed of three superimposed smaller doublets corresponding to a total of 6 methyl groups (the central amide group and one amide group on each of the outer phosphorus atoms) and (c) a doublet due to the remaining 2 amide groups at 2.65 ppm (J_{PH} = 9.0 Hz). The same converging of signals at low T as in ^{31}P spectra is observed, the greatest shift being experienced by the imido signal. The imido protons would indeed be the most sensitive to conformational changes, as is also apparent from a change in solvent (shifts in $(CD_3)_2CO$: (a) 2.87 ppm, (b) 2.71 ppm, (c) 2.65 ppm) and from the La-induced complexation shifts: 0.1 ppm for the quartet, 0.06 ppm for the doublets.

Isotropic shifts induced by the paramagnetic lanthanides were obtained by subtracting the shifts

TABLE IV. Isotropic Shifts [ppm] of the Paramagnetic TRIPA Complexes.

Metal	T [°C]	$\delta(^1H)$			$\delta(^{31}P)$	
		(a)*	(b)*	(c)*	doublet	triplet
Ce	−10	0.10	0.04	−0.08	20.90	−0.25
	−30	0.08	−0.04	−0.02	22.74	−1.16
Pr	−10	0.29	0.09	−0.35	57.72	10.33
	−30	0.34	0.09	−0.34	63.29	10.00
Nd	−10	0.22	−0.07	−0.01	76.89	22.48
	−30	0.20	0.03	0.00	85.09	22.48
Eu	25 °C**				−111.54	−77.29

*(a) denotes the quartet, (b) the broad doublet covering six methyl groups and (c) the smaller doublet covering four methyl groups. **At lower temperatures the two broad ^{31}P signals split up gradually to give nine signals of equal intensity, which cannot be correlated unambiguously to the former doublet–triplet pattern.

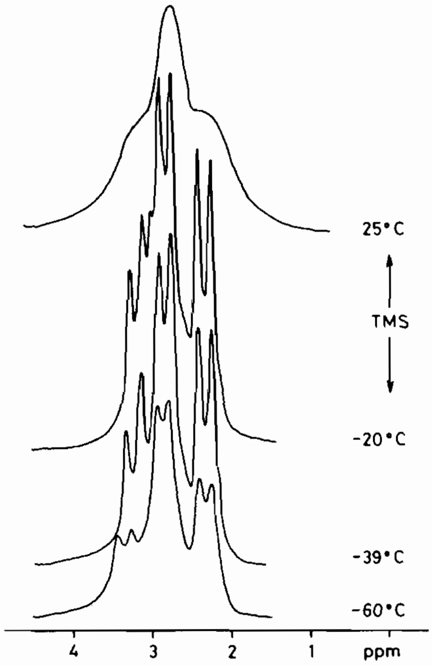

Fig. 4. ^{1}H spectra of the praseodymium complex as a function of temperature.

of the corresponding nuclei in the diamagnetic complexes (the La-complex was used from Ce to Sm, the Lu-complex from Eu to Yb) from the total shifts measured relative to the usual references. In view of the structural changes that occur along the series, the isotropic shifts thus calculated contain some error. The surprisingly small paramagnetic shifts of the ^{1}H signals for the lighter lanthanides (Table IV) may thus bear little significance as to their sign, since they are of the same order of magnitude as the complexation shifts for the diamagnetic lanthanides. The ^{31}P signals, on the other hand, both experience large isotropic shifts. This is an indication that in solution, as well as in the solid state, all PO groups coordinate to the metal ion. The persistence of the doublet-triplet pattern at low T (–70 °C) for Ce, Pr and Nd-complexes furthermore points to a highly symmetric complex structure, TCTP rather than CSAP. While the proton shifts may be due almost entirely to a pseudo-contact interaction [13], the ^{31}P shifts are probably mainly contact shifts [14] and can thus be used as a comparative measure for the Ln–O(P) bond strength. The much smaller shift of the triplet as compared to the doublet confirms the assumption of the central phosphoryl groups being farther away from the metal ion, *e.g.* kept in the capping positions of a TCTP-type coordination sheath.

At higher temperatures the resonances of the praseodymium (and, to a lesser extent, of the cerium) complex show appreciable exchange broadening and converge toward each other (Fig. 4). Considering that a varying excess of free ligand has no visible effect on linewidths or shifts, as checked with ^{31}P spectra, intermolecular ligand exchange can be ruled out. Intramolecular exchange, on the other hand, suggests that conformational exchange does not stop when TRIPA is fixed upon a lanthanide ion. This is consistent with the wide-spread belief in a highly fluxional coordination sphere for lanthanide ions [15]. In order to minimize exchange contributions, isotropic shifts were measured at reasonably low temperature (Table IV). Very low temperatures are characterized by strong paramagnetic signal broadening and were avoided. It is possible, however, that the smallness of the proton shifts (as compared *e.g.* to HMPA complexes [16]: Ce, 1.5; Pr, 3.0; Nd, 1.15 ppm) is partly due to exchange effects.

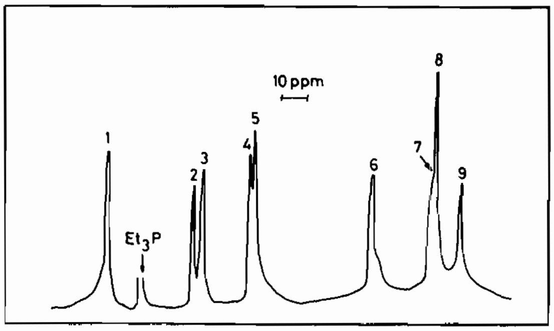

Fig. 5. ^{31}P spectrum of the europium complex at –30 °C (external reference: Et$_3$P).

For the complexes from Sm to Yb no isotropic shifts could be calculated because extensive paramagnetic signal broadening and/or signal multiplication precluded any correlation with the observed diamagnetic resonance pattern. Signal multiplication may be due to symmetry breakdown (*e.g.* increasing distortion of TCTP) or simply to greater sensitivity of the spectra of heavier lanthanides to structural differences. Heavier lanthanides indeed show greater shifting power and slower exchange kinetics than the lighter ones. The ^{31}P spectrum of the europium complex (Fig. 5) thus splits into nine components of more or less equal intensity at lower T, suggesting a totally asymmetric complex structure with nine non-equivalent phosphoryl groups. In one case at least, Dy, the number of phosphorus signals exceeds nine, which we believe is again an indication that more than one complex structure is possible. This correlates with the observed intramolecular exchange described above.

In general, both up- and downfield shifts are observed within the same ^{1}H spectrum, supporting the theory of prevailing pseudo-contact interaction for protons. The shift sign for ^{31}P signals changes at Eu (Ce–Sm: downfield, Eu–Yb: upfield) according to contact shift parameters [17]. On the basis of the largest shift in each spectrum at –30 °C one can deduce the following isotropic shift sequence for protons: Tm(−86) > Er(−39) > Yb(17) ≥ Eu(15) > Sm(1.9) > Pr(0.34) ≥ Nd(0.20) ≥ Ce(0.08) and for phosphorus: Dy(−609) > Tm(−422) ≅ Ho(−400) > Er(−304) > Eu(−163) > Nd(85.09) > Pr(63.29) > Ce(22.74) > Sm(5.5)

The paramagnetic line-broadening follows a similar sequence: Tm > Er > Ho > Dy > Yb > Eu > Sm > Nd > Pr, Ce. As a consequence, spin–spin coupling can only be observed for Pr and Ce complexes. It is noteworthy that no phosphorus–proton spin decoupling occurs as in the HMPA complexes of paramagnetic d metals [18]. This may be due to the much smaller scalar coupling constant associated with a Ln–O(P) bond [19].

Conclusion

We have synthesized the first series of lanthanide complexes with the general formula $[\mathrm{LnL_3}](\mathrm{ClO_4})_3$, where L is a neutral tridentate phosphoryl ligand. All PO groups coordinate, giving a nine-coordinate complex structure which goes through subtle changes along the series, both in solution and in the solid state. These changes are described in terms of conformational modifications occurring in the complexed ligand molecules and entailing structural changes in the overall coordination sphere. An ideal polyhedron is probably only approximated for the lighter lanthanides. The complexes are quite inert with respect to ligand exchange.

Acknowledgments

I am indebted to M. Donald Zbinden and Miss Lale Hatiboglu for helping out in the experimental part. This work was supported by the Swiss National Science Foundation through grant No. 2.921-0.77.

References

1 M. W. G. de Bolster and W. L. Groeneveld, *Recueil Trav. Chim.*, *91*, 171 (1972).
2 R. P. Scholer and A. E. Merbach, *Inorg. Chim. Acta, 15,* 15 (1975); J. T. Donoghue, E. Fernandez, J. A. McMillan and D. A. Peters, *J. Inorg. Nucl. Chem.*, *31*, 1431 (1969); E. Giesbrecht and L. B. Zinner, *Inorg. Nucl. Chem. Letters*, *5*, 575 (1969).
3 C. Airoldi, Y. Gushikem, and C. R. Puschel, *J. Coord. Chem.*, *6*, 17 (1976).
4 M. W. G. de Bolster, J. den Heijer and W. L. Groeneveld, *Z. Naturforsch.*, *276*, 1324 (1972).
5 W. J. J. M. Sprangers, *Ph.D. Thesis*, Leiden (1975); R. Louw, private communication (1978).
6 J. E. Gardiner and B. A. Kilby, *J. Chem. Soc.*, 1769 (1950).
7 P. Lester, U.S. 2 678 335, *Chem. Abstr.*, *49*, 6300 (1955).
8 R. L. Arceneaux, J. G. Frick, Jr., E. K. Leonard and J. D. Reid, *J. Org. Chem.*, *24*, 1419 (1958).
9 A. A. Zinov'ev and N. A. Shchirova, *Russ. J. Inorg. Chem.*, *5*, 626 (1960).
10 J. Körbl, R. Pribil and N. A. Emr, *Z. anal. Chem.*, *156*, 292 (1957); G. Brunisholz and M. Randin, *Helv. Chim. Acta*, *42*, 1932 (1959).
11 M. W. G. de Bolster and W. L. Groeneveld, *Recueil Trav. Chim.*, *90*, 477 (1971); *ibid.*, *90*, 687 (1971); *ibid.*, *91*, 95, 171, 185, 643 (1972).
12 M. G. B. Drew, *Coord. Chem. Rev.*, *24*, 179 (1977).
13 C. D. Barry, J. A. Glasel, A.C.T. North, R. J. P. Williams, and A. V. Xavier, *Nature*, *232*, 236 (1971).
14 C. M. Dobson, R. J. P. Williams and A. V. Xavier, *J. Chem. Soc. Dalton*, 2662 (1973).
15 R. C. Fay, D. G. Lewis and J. R. Weir, *J. Am. Chem. Soc.*, *97*, 7179 (1975) and references cited therein.
16 J. Briggs, G. H. Frost, F. A. Hart, G. P. Moss and M. L. Staniforth, *Chem. Comm.*, 749 (1970).
17 J. Reuben and D. Fiat, *J. Chem. Phys.*, *51*, 4909 (1969).
18 B. B. Wayland and R. S. Drago, *J. Am. Chem. Soc.*, *87*, 2372 (1965); T. Chen and L. O. Morgan, *J. Phys. Chem.*, *76*, 1973 (1972).
19 A. A. Pinkerton and W. L. Earl, *J. Chem. Soc. Dalton*, 267 (1978).